CONCEPTUAL DESIGN OF A LUNAR BASE THERMAL CONTROL SYSTEM

Lisa C. Simonsen

NASA Langley Research Center
Hampton VA 23665-5225

Marc J. DeBarro

Rockwell International
12214 Lakewood Blvd.
Downey CA 90241

Jeffery T. Farmer

NASA Langley Research Center
Hampton VA 23665-5225

Space station and alternate thermal control technologies were evaluated for lunar base applications. The space station technologies consisted of single-phase, pumped water loops for sensible and latent heat removal from the cabin internal environment and two-phase ammonia loops for the transportation and rejection of these heat loads to the external environment. Alternate technologies were identified for those areas where space station technologies proved to be incompatible with the lunar environment. Areas were also identified where lunar resources could enhance the thermal control system. The internal acquisition subsystem essentially remained the same, while modifications were needed for the transport and rejection subsystems because of the extreme temperature variations on the lunar surface. The alternate technologies examined to accommodate the high daytime temperatures incorporated lunar surface insulating blankets, heat pump system, shading, and lunar soil. Other heat management techniques, such as louvers, were examined to prevent the radiators from freezing. The impact of the geographic location of the lunar base and the orientation of the radiators was also examined. A baseline design was generated that included weight, power, and volume estimates.

INTRODUCTION

Permanent manned presence on the Moon has been identified by the National Commission on Space as one of the bold new initiatives beyond the space station to explore and settle the solar system (*Ride*, 1987). Accordingly, a joint systems study between NASA Langley Research Center (LaRC) and NASA Johnson Space Center (JSC) was conducted to aid in determining the appropriate systems required by man to survive for extended durations on the lunar surface. The thermal control system (TCS) was identified as a key element for the efficient operation of the lunar base.

This paper discusses the major elements of a conceptual design of a lunar base thermal control system. Both passive and active options were considered for temperature control in the manned sections of the base. The extreme variations of the lunar surface temperature in the lower latitudinal regions were addressed in the conceptual design. Space station thermal control technology was used as the baseline in developing the thermal control design.

LIST OF SYMBOLS

H	Height (m)
h	Heat Transfer Coefficient (W/m^2-K)
k	Thermal Conductivity (W/m-K)
P	Pressure (kPa)
Q	Heat (kW)
q	Heat Flux (W/m^2)
r	Radius (m)
T	Temperature (K)
α	Absorptivity
ϵ	Emissivity
γ	Angle of Incidence of the Solar Flux on the Radiator (Deg.)
η_c	Isentropic Efficiency
ϕ	Latitude (Deg.)
σ	Stefan-Boltzmann Constant
Θ	Angle Sun is Above Lunar Horizon (Deg.)

subscripts:

Al	Aluminum
N	Normal
rad	Radiator
reg	Regolith
sink	Environmental Sink
1	Inner Module Wall
2	Surface of MLI
3	Inner Surface of Aluminum Structure
4	Outer Surface of Aluminum Structure
5	Lunar Surface

APPROACH

The configuration of the lunar base habitat was designed to meet requirements established by JSC. The impact of the lunar environment on the habitat and the proposed activities in the facility were evaluated to determine design specifications for the thermal control system.

A baseline configuration for the thermal control system was developed using the current space station thermal control technologies. The acquisition technology for the internal heat

loads in the space station consists of single-phase, pumped water loops that operate at temperatures of 2°C and 21°C for sensible and latent heat removal. A two-phase ammonia loop transports the heat from the modules to a series of individual ammonia heat pipe radiators (*NASA*, 1984). Passive thermal control was assumed to consist primarily of standard multilayer insulation.

If the space station technology proved inadequate for lunar application, it was either modified to accommodate the lunar environment or replaced by an alternate technology. Using this approach, the thermal control systems for the first phases of a permanent lunar base were established using as many known and tested technologies as applicable. Thermal control system summaries for the habitable areas of the lunar base were then generated using information available on the technologies selected.

LUNAR BASE DESCRIPTION

A lunar base functional analysis received from JSC was used to determine the habitat and laboratory facilities required to sustain base operations. Two phases of the lunar base were addressed, an initial phase and a growth phase. The initial phase will support preliminary exploration and limited materials research. The facilities will be operated by a crew of 4 for approximately 10 Earth days. The growth phase will have facilities for larger scale materials research, closed-loop research, and liquid oxygen utilization. This phase will be permanently manned with a crew of eight.

The habitat and laboratory facilities were assumed to be constructed entirely from space station modules, nodes, and airlocks. Modules were 4.5 m in diameter by 13.3 m long. Nodes were 4.5 m in diameter by 6.0 m long. Both were aluminum cylindrical structures. An airlock was an aluminum sphere 3.7 m in diameter. The initial phase consisted of a habitat module, three nodes, and three airlocks. The growth phase consisted of two habitat modules, a laboratory module, six nodes, four airlocks, and an observatory. The configurations for the two phases are shown in Fig. 1. A space station node was used to model the observatory. The base was assumed to be either under a supporting structure covered by 2 m of lunar regolith or directly buried under 2 m of lunar regolith. Approximately 2 m of lunar regolith was estimated as sufficient to protect the crew from cosmic radiation (*Duke et al.*, 1985).

The Solar System Exploration Division at JSC identified four possible sites for the first base. They were Lacus Veris (87.5°W, 13°S), the South Pole, the Apollo 17 landing site (30°E, 20°N), and the Mare Nubium (10°W, 10°S).

LUNAR ENVIRONMENT

The lunar environment changes dramatically from day to night and from location to location. The lunar day lasts approximately 28 Earth days with 14 days of sunlight and 14 days of darkness. The lunar surface temperature can range from 374 K during the lunar noon (Earth day 7) to 120 K during the lunar night. Figure 2 shows the temperature variations over the lunar day at different latitudes. These plots were generated using an empirically derived equation from *McKay* (1963). The equation was modified to include the effects of the varying solar flux at different latitudes resulting in the following

$$T_{moon}\,(K) = 373.9(\cos\phi)^{.25}(\sin\theta)^{.167}$$

In addition, features of the lunar environment could protect a lunar base from these severe temperature variations. For example, there may be permanently shadowed regions near the poles that have consistently low temperatures (*Stimpson and Lucas*, 1972). The lunar regolith could be used as thermal protection because it is an excellent insulator with an average thermal conductivity of approximately 0.004 W/m-K (*Dalton and Hohmann*, 1972). The regolith immediately below the lunar surface could provide a stable thermal gradient that is relatively insensitive to the day/night surface temperature variations. The utilization of these features could enhance a TCS design.

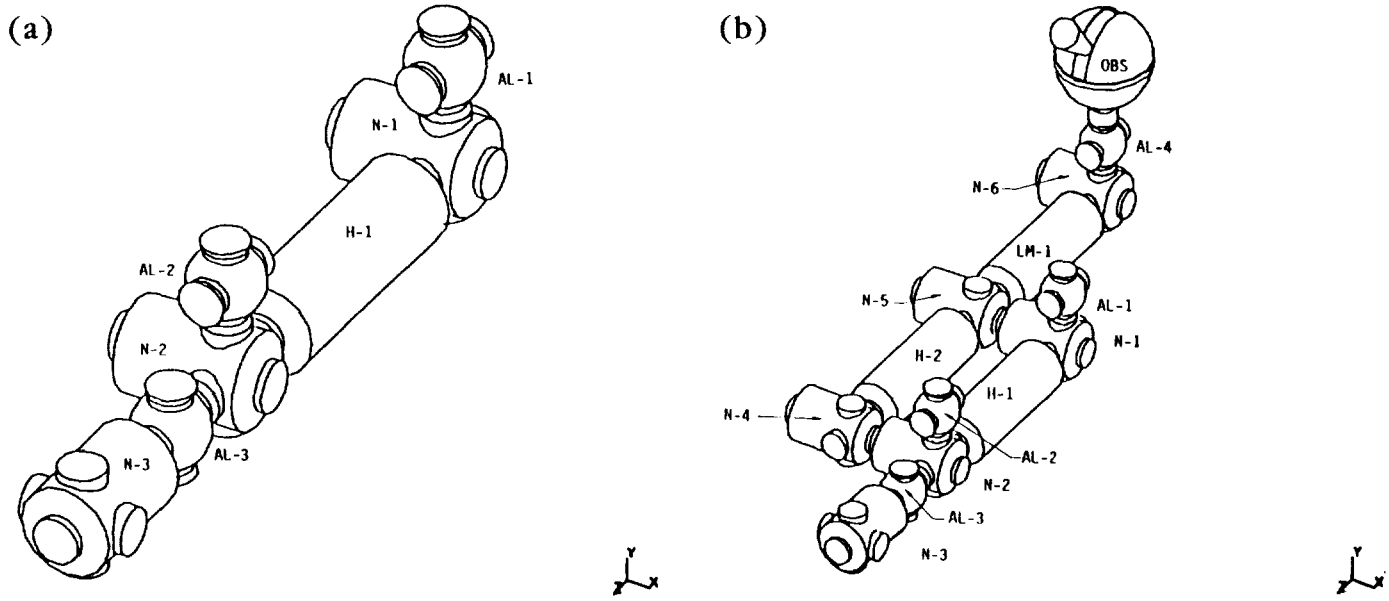

Fig. 1. Lunar base module configurations.

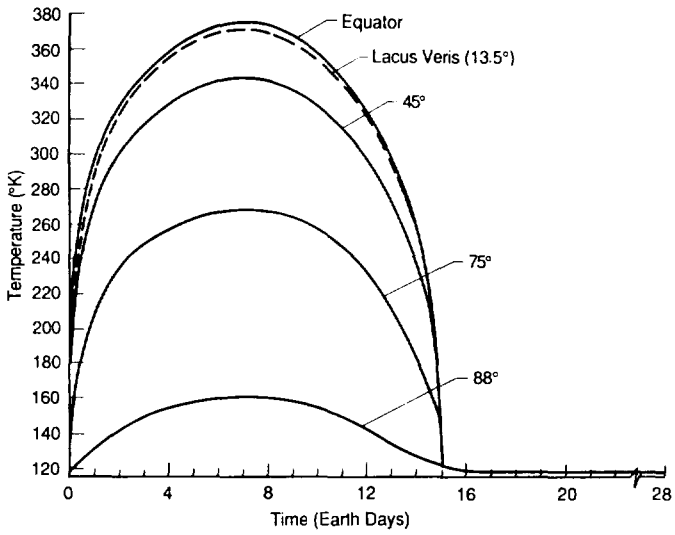

Fig. 2. Lunar surface temperature profile at different latitudes.

THERMAL CONTROL REQUIREMENTS

The TCS for the habitable areas of the base was designed to maintain the temperature inside the modules between 18°C and 24°C and to maintain the dew point temperature between 4°C and 16°C. To accomplish this, the equipment and metabolic heat loads must be actively removed, and the external gains and losses must be minimized.

The total heat loads assigned to each module, node, and airlock were selected based upon the specified load requirements of the space station (*NASA*, 1984). These loads are listed in Table 1 for heat acquired at 2°C and 21°C. Included in these loads are the metabolic sensible (crew) and latent (humidity) heat, as listed in Table 2.

The external heat gains and losses between the modules and the environment were calculated for three cases to determine if additional load requirements would be imposed upon the active thermal control system. The three cases considered were (1) a module protected under an aluminum supporting structure with 2 m of regolith on top, (2) a module directly buried under 2 m of regolith, and (3) a module directly on the lunar surface. The heat gains and losses of the modules protected with 2 m of regolith were negligible for modules both at the lower latitudinal sites (Lacus Versis, Apollo 17, and Mare Nubium) and at the South Pole. However, for a module directly on the surface (i.e., the observatory) at the lower latitudinal sites, there will be an added load of 2.2 kW heat gain during the hottest part of the lunar day, and there will be a heat loss of 1.7 kW during the night. For a module on the surface at the South Pole, there will be a heat loss over the entire day with a maximum heat loss at night of 1.7 kW. These added loads will be addressed in the design of the acquisition system. The details of the analysis are explained in the Appendix.

Using the heat loads listed in Table 1 for all the base modules, excluding node 3 (assumed to be a logistics module with no active TCS) and airlock 4 (used as access to the observatory with no active TCS), the maximum heat load for the initial phase is 65 kW at 21°C and 30 kW at 2°C. Likewise, the maximum heat load for the growth phase is 135 kW at 21°C and 66 kW at 2°C.

CONCEPTUAL DESIGN

The Lacus Veris, Apollo 17 landing, and the Mare Nubium sites experience essentially identical thermal environments because of their similar distances from the equator. Therefore, one TCS designed for the lower latitudinal regions could be used at all three sites. Since the lunar surface temperature variations become less pronounced at higher latitudes, the South Pole site will experience a different, more benign environment. Therefore, a separate TCS design may be needed.

Conceptual TCSs were designed to acquire the heat loads and reject them into the lunar environment for the South Pole and the lower latitudinal sites. The internal thermal requirements for the base at these locations were essentially identical. However, since the rejection environments are unique to location, the rejection systems for the South Pole and the lower latitudinal sites were evaluated separately.

Acquisition Considerations and System Design Estimates

The ambient environment in the lunar base modules and the heat loads acquired in the modules were similar to those projected for the space station modules; therefore, the space station's acquisition technology was used for the lunar base. However, the weight, volume, and power distributions were different because of the configuration of the base modules and the layout of the acquisition system.

Each module's acquisition system was sized to accommodate the heat loads specified in Table 1, although this capacity was not immediately required. Included in these loads was 2.36 kW for each air temperature and humidity control system designed to remove metabolic sensible and latent heat loads (Table 2) and to cool equipment in case of emergency.

The air temperature and humidity control heat loads were charged to node 1 for the initial phase and to nodes 5 and 6 for the growth phase. Two relative humidity and sensible heat exchangers will remain in operation in nodes 1 and 5, while the relative humidity and sensible heat exchangers in node 6 will be used to meet safe haven requirements. If the base were located at a lower latitudinal site, the unit in node 6 would also be used

TABLE 1. Selected heat loads in the habitable areas.

Module	Heat Load (kW/module) 2°C	21°C
Habitation Module	10	15
Laboratory Module	10	15
Node	4	10
Airlock	4	10
Observatory	4	10

TABLE 2. Metabolic sensible and latent heat loads.

Type	Load	
Metabolic Sensible	0.086	kW/man
Latent		
Sweat and respiration water	1.82	kg/man day
Hygiene water	0.44	kg/man day
Food preparation water	0.03	kg/man day
Experiment water	0.45	kg/man day
Laundry water	0.06	kg/man day

to provide the observatory with the added cooling and heating requirements during the hottest and coldest times of the lunar day. If the base were located at the South Pole, the heat exchangers would need to provide additional heating during the entire lunar day/night to compensate for the heat losses to the environment.

The remaining module heat loads were accommodated by cold plates designed to meet all normal equipment cooling requirements and customer needs. The cold plates are arranged in parallel to provide isothermal operating conditions (Fig. 3). The cold plates are stainless steel and are cooled by either the 2°C or 21°C pumped water loop. The available cold plates in each module are listed in Table 3.

The module heat loads were pumped to the bus heat exchangers located near the main transport line. Some modules contain support loops to pump the heat acquired in one location through another module to the bus heat exchanger to reduce the lengths of external transport lines. A typical layout is shown in Figs. 4a and 4b for the initial and growth phases, respectively. Weight, volume, and power estimates for the acquisition systems in the initial and growth configurations are shown in Tables 4 and 5, respectively.

The weight, volume, and power estimates were computed using the Emulation-Simulation Thermal Control Model for Space Station Application developed by LaRC and Georgia Institute of Technology (*Hall et al.,* 1986; *Colwell and Hartley,* 1988) and data obtained from Marshall Space Flight Center (MSFC). Estimates for the air temperature and humidity control system contained relative humidity and sensible heat exchangers, a water separator, and redundant water transport lines operating at 2°C. It also included a ventilation system composed of ducting, intake filters, and fan packages. The above estimates for the equipment heat acquisition loops contained cold plates, redundant pump packages, redundant liquid water transport loops, disconnects, valves, flex hoses, controllers, transducers, sensors, etc. The above estimates for the support loops contained redundant transport lines, fittings, controllers, disconnects, transducers, and sensors.

Heat Rejection Considerations

The acquired heat loads on the space station are transported from the module bus heat exchangers via separate pumped two-phase ammonia loops at 2°C and 21°C to aluminum heat pipe radiators. An 8° temperature drop was assumed between the acquisition cold plates and the heat pipe radiators, resulting in radiator rejection temperatures of -6°C and 13°C. In the space station environment, the radiators can be oriented to reject an average of 100 W/m^2 at -6°C and 160 W/m^2 at 13°C.

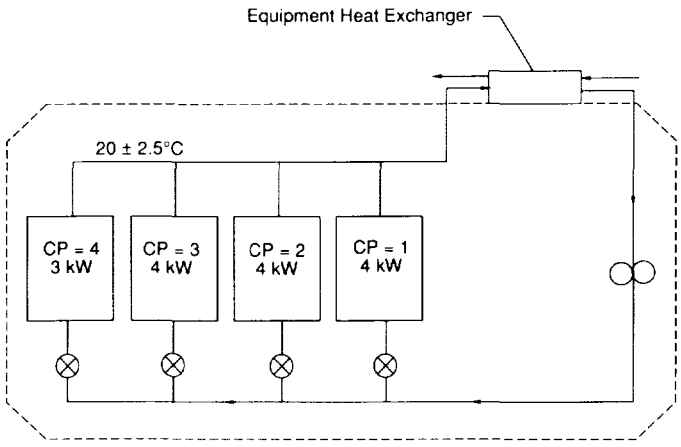

Fig. 3. Typical cold plate configuration for an integrated module.

TABLE 3. Equipment loads in each module.

Module	Temp of Loop (°C)	Number of Cold Plates	Load on Each (kW) 1	2	3	4
Habitation	2	3	2.0	4.0	4.0	0.0
	21	4	4.0	4.0	4.0	3.0
Laboratory	2	3	2.0	4.0	4.0	0.0
	21	4	4.0	4.0	4.0	3.0
Node (2,4)	2	2	2.0	2.0	0.0	0.0
	21	4	2.5	2.5	2.5	2.5
Node (1,5,6)	2	1	1.6	0.0	0.0	0.0
	21	4	2.5	2.5	2.5	2.5
Airlock (1,2,3)	2	2	2.0	2.0	0.0	0.0
	21	3	5.0	2.5	2.5	0.0
Observatory	2	2	2.0	2.0	0.0	0.0
	21	4	2.5	2.5	2.5	2.5

The thermal environment is more severe on the lunar surface, resulting from direct solar flux and infrared (IR) flux from the lunar surface. These factors degrade the average heat rejection capability of the radiators. In some instances these effects prevent the radiators from emitting heat and may cause them to gain heat from the external environment.

The rejection capability of the radiators was estimated using the following equation

$$q = \epsilon\sigma(T^4_{rad} - T^4_{sink})$$

where q is the radiator heat rejection capability in W/m^2 and T_{sink} is the effective environmental temperature (K). The sink temperature represents the added effects of cold space, solar flux, and IR flux from the lunar surface. The sink temperature calculations were based on the methodology presented in *Dallas et al.* (1971). They will depend on the latitude and orientation of the radiators, the time of day, and the radiator's surface properties. The radiators in this analysis were assumed to have an end-of-life emissivity of 0.80 and an absorptivity of 0.30 (*NASA,* 1984).

Computer programs were generated to calculate the variations in the heat rejection capability of the radiators over the lunar day for various orientations at different latitudes. Three orientations were considered. They included (1) a vertical radiator perpendicular to the plane of the solar ecliptic, (2) a vertical radiator parallel to the plane of the ecliptic, and (3) a horizontal radiator insulated from the lunar surface (Fig. 5). The total heat rejection capability calculated in the program represented the amount of heat per square meter of radiator panel. That is, if a vertical two-sided radiator had a heat flux of 200 W/m^2, it would reject 100 W/m^2 per side. Likewise, if a horizontal radiator had a heat flux of 200 W/m^2, it would reject 200 W/m^2 from one side. If a positive heat flux were calculated, the radiator would radiate heat to the environment. If, however, a negative heat flux were calculated, the radiator would gain heat. These conventions are shown in Fig. 6.

Heat rejection at the South Pole. Figure 7 shows radiator heat rejection capability over the lunar day and night for radiator wall temperatures of -6°C and 13°C. Figure 7a indicates that horizontal radiators would provide the base with a capability that is continuously above the 100 W/m^2 average rejection capability of a space station radiator at -6°C. The other orientations fall

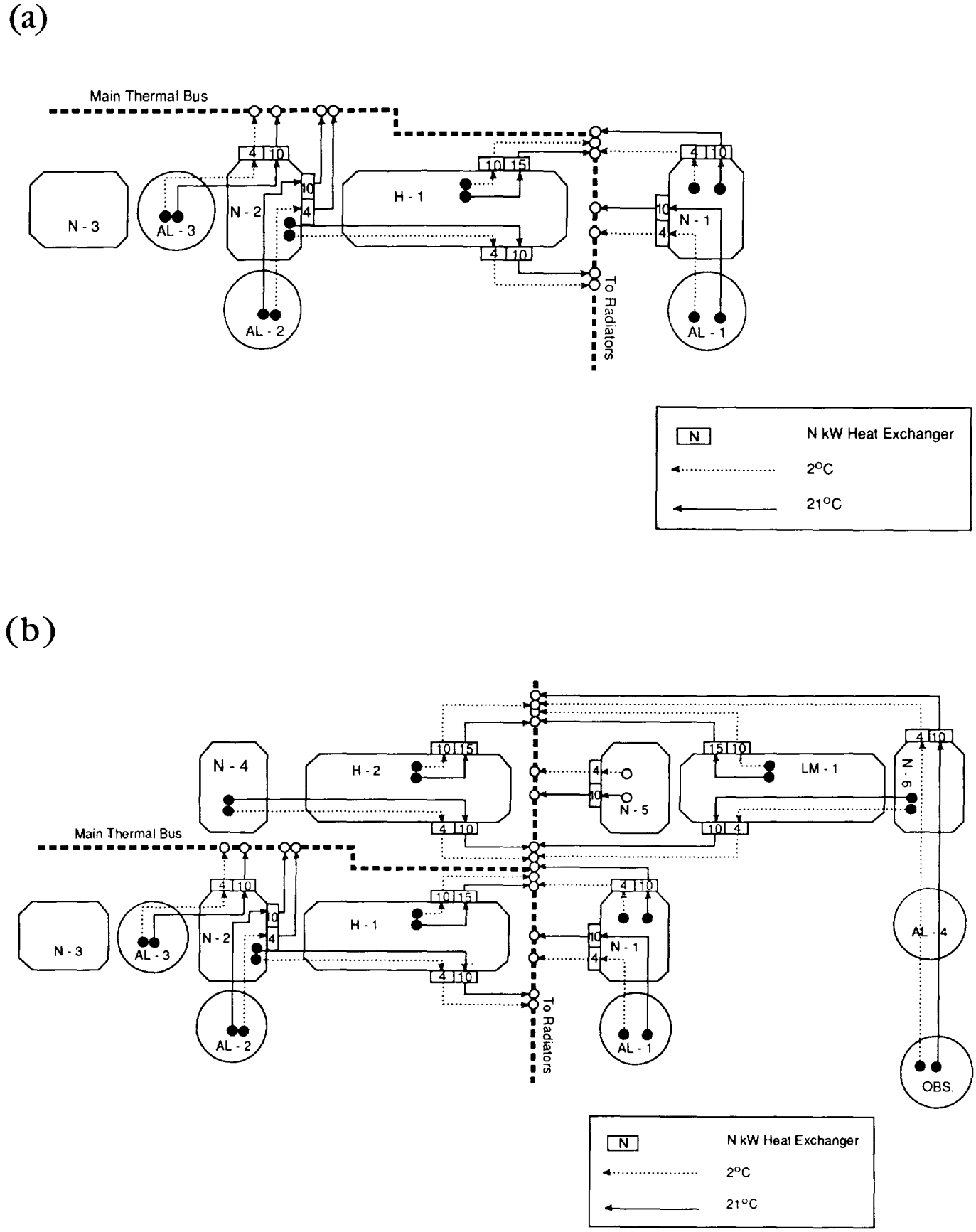

Fig. 4. **(a)** Initial phase layout of acquisition system. **(b)** Growth phase layout of acquisition system.

TABLE 4. Acquisition summary: Initial phase.

Item		Habitation Module-1	Node-1	Node-2	Air Lock-1	Air Lock-2	Air Lock-3
Weight (kg)							
Air Temperature and Humidity Control		149	143	57	57	57	57
Equipment Heat Acquisition	2°C	355	68	104	100	100	100
	21°C	390	200	191	195	195	195
Support Loop	(2°C and 21°C)	81	73	146	0	0	0
Total		975	484	498	352	352	352
Volume (m^3)							
Air Temperature and Humidity Control		1.73	0.71	0.40	0.40	0.40	0.40
Equipment Heat Acquisition	2°C	0.21	0.07	0.09	0.08	0.08	0.08
	21°C	0.22	0.10	0.10	0.10	0.10	0.10
Support Loop	(2°C and 21°C)	0.04	0.03	0.07	0	0	0
Total		2.20	0.91	0.66	0.58	0.58	0.58
Power (kW)							
Air Temperature and Humidity Control		0.49	1.04	0.15	0.15	0.15	0.15
Equipment Heat Acquisition	2°C	0.32	0.02	0.07	0.07	0.07	0.07
	21°C	0.29	0.18	0.18	0.19	0.19	0.19
Support Loop	(2°C and 21°C)	0.03	0.03	0.06	0	0	0
Total		1.13	1.27	0.46	0.41	0.41	0.41

TABLE 5. Acquisition summary: Growth phase.

Item		Habitation Module-2	Laboratory Module-1	Node-3	Node-4	Node-5	Node-6	Air Lock-4	Observ-atory
Weight (kg)									
Air Temperature and Humidity Control		149	149	57	57	143	143	57	57
Equipment Heat Acquisition	2°C	355	355	0	104	68	68	0	104
	21°C	390	390	0	191	191	191	0	191
Support Loop	(2°C and 21°C)	81	81	0	0	0	146	46	0
Total		975	975	57	352	402	548	103	352
Volume (m^3)									
Air Temperature and Humidity Control		1.73	1.73	0.40	0.40	0.71	0.71	0.40	0.40
Equipment Heat Acquisition	2°C	0.21	0.21	0	0.09	0.07	0.07	0	0.09
	21°C	0.22	0.22	0	0.10	0.10	0.10	0	0.10
Support Loop	(2°C and 21°C)	0.04	0.04	0	0	0	0.07	0.02	0
Total		2.20	2.20	0.40	0.59	0.88	0.95	0.42	0.59
Power (kW)									
Air Temperature and Humidity Control		0.48	0.48	0.15	0.15	1.04	1.04	0.15	0.15
Equipment Heat Acquisition	2°C	0.32	0.22	0	0.07	0.02	0.02	0	0.07
	21°C	0.29	0.29	0	0.18	0.18	0.18	0	0.18
Support Loop	(2°C and 21°C)	0.03	0.03	0	0	0	0.06	0.03	0
Total		1.13	1.13	0.15	0.40	1.24	1.30	0.18	0.40

below the 100 W/m^2 level during periods of large solar and IR fluxes. Figure 7b indicates that the radiator rejection capability for all orientations is above the 160 W/m^2 average rejection capability of a space station radiator at 13°C. The heat rejection for the horizontal radiator configuration also provides a comparatively constant flux.

The results of this analysis indicate that a space station-type radiator assembly with a horizontal radiator orientation could accommodate the thermal environment of the South Pole without any major modifications or enhancements to the system.

Heat rejection at lower latitudinal sites. The rejection capabilities for three radiator orientations with a -6°C wall temperature and a 13°C wall temperature at Lacus Veris are shown in Figs. 8a and 8b, respectively. As indicated by the figures, none of the orientations for either temperature loop provides a capability that meets the 100 W/m^2 level for the entire day. In fact, the heat fluxes become negative for large portions of the lunar day. The heat gain experienced by the radiators can lead to elevated radiator temperatures and thermal control disfunction.

Two possible enhancements to improve rejection capability were identified. The first was to lower the sink temperature by using reflective insulating blankets, which reduce the lunar IR flux on the radiators. The second was to elevate the rejection temperature above the sink temperature using a heat pump assembly. Thermal storage was considered; however, the large heat loads for long durations would result in a massive system using current storage technology (*NASA*, 1985). The use of lunar regolith for thermal storage may require extremely large heat transfer areas because of its low conductance.

The lunar heat flux affecting a vertical radiator's rejection capability is a function of the lunar surface temperature, the view factor of the radiator to the surface, and the radiator emissivity.

By covering the surface in the proximity of the radiator with highly reflective, low solar absorptivity blankets, the lunar surface temperature can be significantly reduced, which may reduce the sink temperature enough below the radiator wall temperature to produce reasonable rejection capability. This surface temperature reduction must be traded against an increase in solar flux, which results from solar radiation reflecting off the blankets onto the radiator surface.

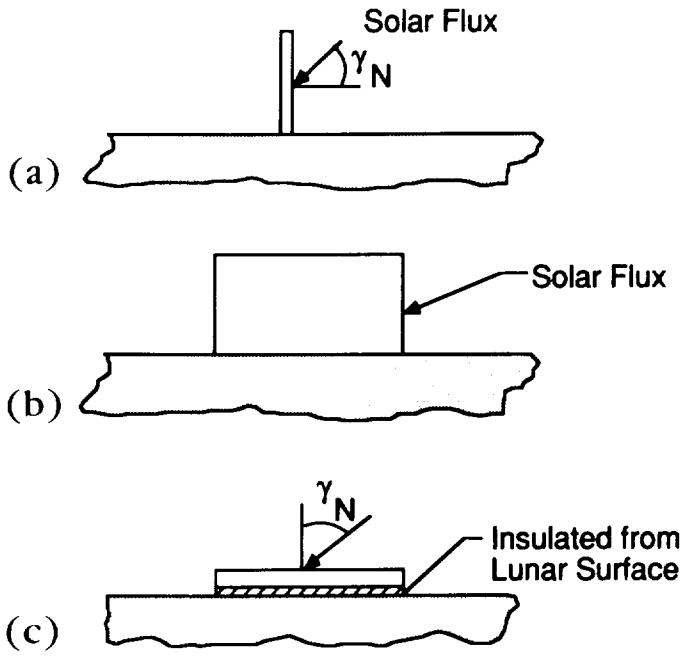

Fig. 5. Radiator orientations.

A computer model was generated to determine the minimum blanket size required to produce favorable sink temperatures. The computer model simulated a vertical, two-sided radiator oriented parallel to the solar ecliptic. Radiator and blanket surface temperatures could be calculated at any latitude on the Moon. The reflective insulating blankets were assumed to be adiabatic, with a very low thermal conductivity. Blanket size was measured on the basis of blanket width to radiator length (W/L), vs. radiator height to radiator length (H/L) as defined in Fig. 9.

From the above model, it was found that the reflective blankets significantly reduced the radiator sink temperature for radiator height to blanket width (H/W) ratios above 0.3 (H/L divided by W/L from Fig. 10). If the insulation area were increased further, only a slight reduction in T_{sink} would occur.

Based on a H/W ratio of 0.3, sink temperatures of radiators surrounded by reflective insulating blankets were calculated at Lacus Veris over the length of the lunar day. The blanket was assumed to have α/ϵ equal to 0.1/0.9. The calculated sink temperatures were compared with those for the uninsulated case, as shown in Fig. 11. From the figure, it is shown that at lunar noon, a 50°C temperature drop is achieved in the sink temperature. However, the sink temperature still remains higher than the low rejection temperature loop, primarily because of the increase in reflected solar flux. Consequently, a radiator heat gain is still present for parts of the lunar day. The insulating blankets do not provide sufficient improvement in the rejection capability.

An alternative to lowering the sink temperature is to raise the radiator temperature significantly above the existing sink temperature. This could be done by using a heat pump system. The system evaluated in this study was a cascaded vapor cycle system (VCS) coupled with standard space station ammonia heat pipe radiators.

A schematic of a two-loop cascaded VCS is shown in Fig. 12 (S. T. Worley, personal communication, 1988). The central bus working fluid enters the VCS in a superheated state and is then further pressurized by the compressor. The refrigerant is then cooled to a saturated liquid state in the evaporator/condensor and then subcooled before finally returning to the central bus. The

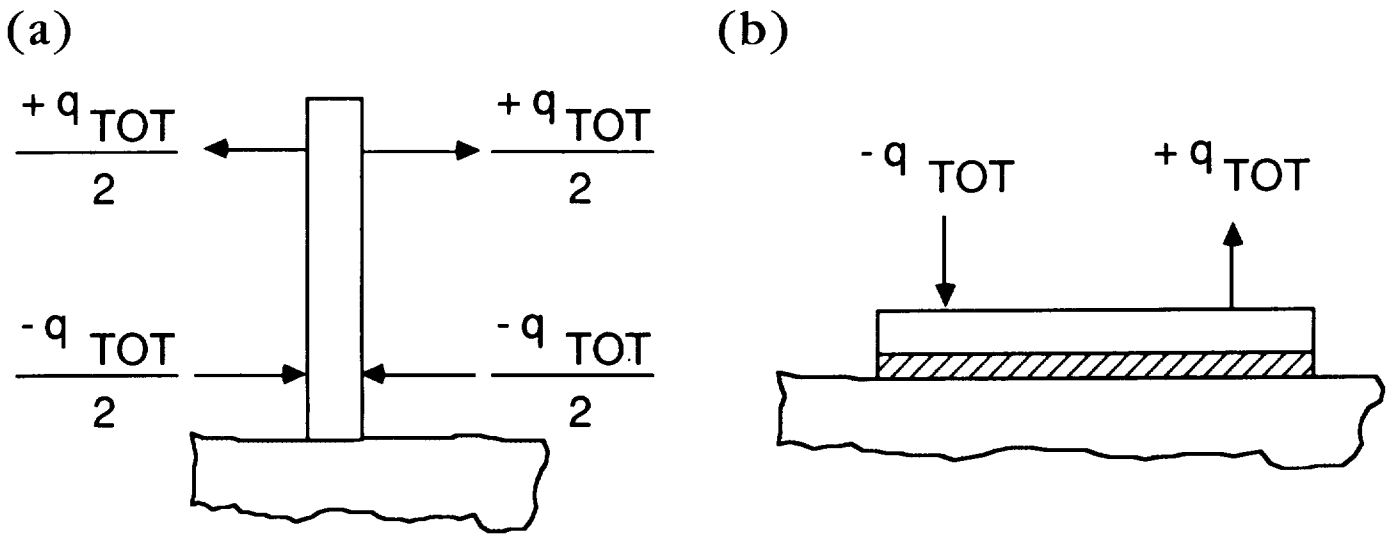

Fig. 6. Heat flux conventions used.

working fluid in the second loop picks up heat in the evaporator/condensor and proceeds through a similar process, where the heat is removed from the radiator at an elevated temperature.

A cascaded VCS was selected over a single-loop VCS to allow for more efficient compression and temperature ratios over the compressors. The refrigerants were selected based on the temperature excursions involved in each loop. The cascaded system would allow for stagewise operation, that is, each added stage could be run as an increased radiator temperature was needed to reject to the increasing sink temperature encountered over the lunar day. This would enable the radiator to operate with a more constant heat flux. The heat rejection capability variations from vertical radiators (parallel to the solar ecliptic) over the lunar day at Lacus Veris are illustrated in Fig. 13. During days 0-2 and days 12-14, the second stage of the cascaded system would be operating while the first-stage compressor was bypassed, during days 3-11 both compressor loops would be in operation, and during days 15-28 no compressors would be in operation.

The coinciding power requirements for the initial phase are shown in Fig. 14. The use of the VCS would increase power requirements by up to 50 kW. The first loop compressor required 20.5 kW and the second loop compressor required 29.5 kW. The use of the VCS would also increase the amount of heat to be rejected. The total heat load to be rejected equals the heat acquired in the habitable areas plus the heat imparted to the working fluid by the compressors. A stagewise operation would, however, minimize the extra power requirements and the extra amount of heat to be rejected during the portions of the lunar day when one or both loops were bypassed.

Table 6 lists the maximum and minimum radiator rejection capabilities (q), areas required for heat rejection, and the total heat loads to be rejected for the initial phase. By selecting a final rejection temperature of 360 K, a midstage loop temperature of 311 K can be obtained for an effective operating range of the system. These temperatures will require similar maximum radiator rejection areas (257, 242, 226 m^2) during minimum rejection

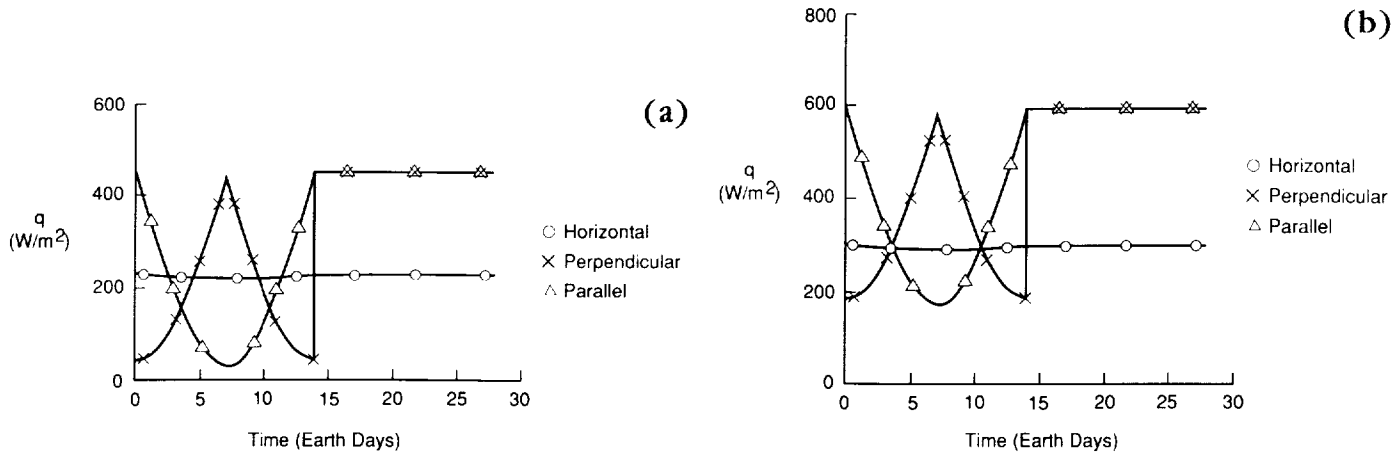

Fig. 7. **(a)** Heat rejection capability for radiators with a wall temperature of -6°C at the South Pole. **(b)** Heat rejection capability for radiators with a wall temperature of 13°C at the South Pole.

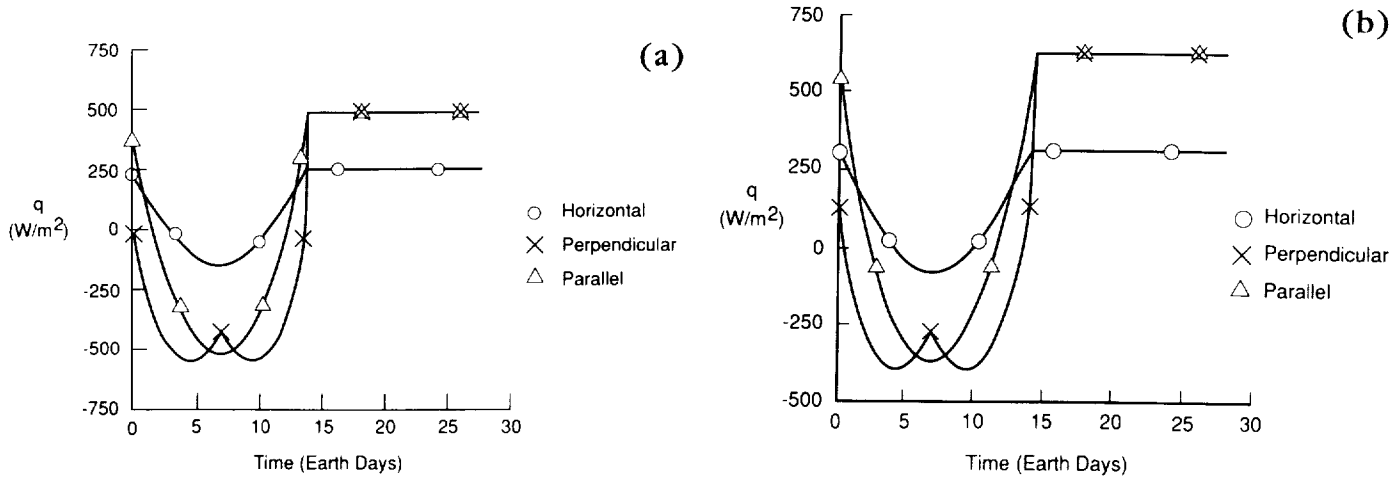

Fig. 8. **(a)** Heat rejection capability for radiators with a wall temperature of -6°C at Lacus Veris. **(b)** Heat rejection capability for radiators with a wall temperature of 13°C at Lacus Veris.

times. This temperature selection would therefore reduce the amount of total radiator area required.

As shown in Fig. 13, the stagewise operation of the VCS still results in fairly wide excursions in the heat rejection capability (420 W/m^2 to 900 W/m^2). Since the area of the radiators is based on the minimum heat rejection capability, the potential exists for a radiator to over-reject during times when the radiator flux is larger than the design level. This can cause thermal and fluid imbalances in the radiator and the rest of the TCS.

A three- or four-stage refrigeration system may be considered as a means to provide a more constant heat flux for the radiators and to further reduce the overall power requirements. However, as the number of refrigeration stages increases, the maintenance and the complexity of the system are expected to increase, and the reliability is expected to decrease. Other means of minimizing the effects of the high peaks on Fig. 13 would be to use louvers or variable conductance heat pipes.

Louvers function by changing the effective α/ϵ ratio of the radiator (*Agrawal*, 1986). This could be accomplished by opening or closing the louver blades over the highly emisssive radiator surface, thereby increasing or decreasing the effective emittance of the radiator. This concept could be used to help reduce the peaks shown in Fig. 13 by closing the louvers (reducing the emittance) during the times when the flux capability is significantly

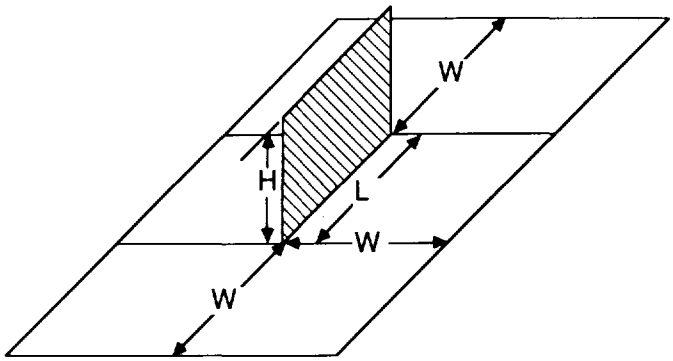

Fig. 9. Radiator and reflective insulation blanket model.

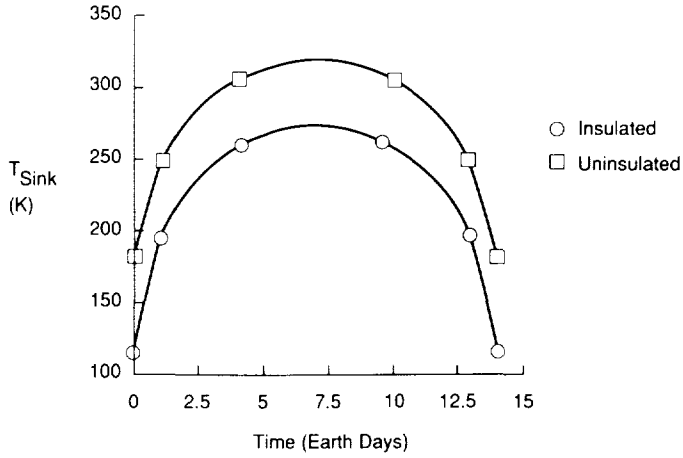

Fig. 11. Uninsulated vs. insulated sink temperatures over the lunar day for a radiator at Lacus Veris.

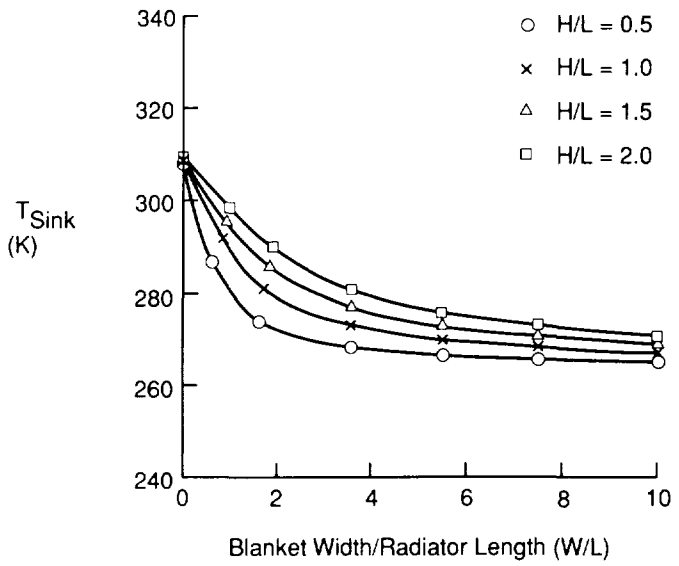

Fig. 10. Effective sink temperatures at noon for a radiator with varying amounts of reflective insulation blankets at Lacus Veris.

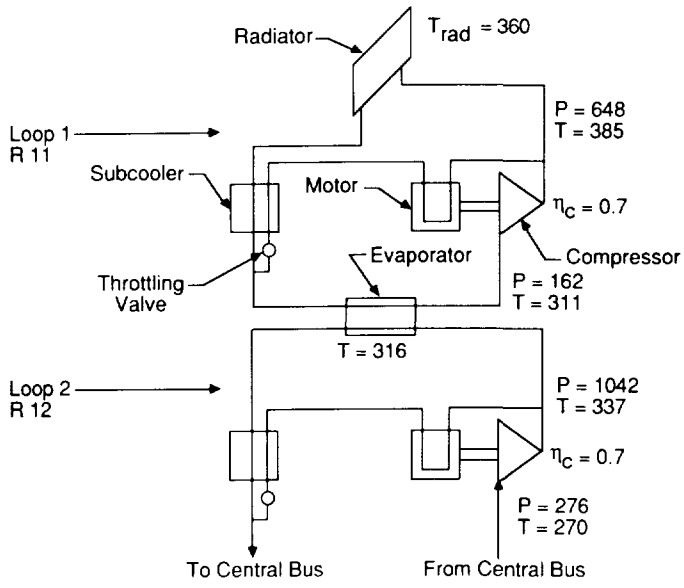

Fig. 12. Two-loop cascaded vapor cycle system.

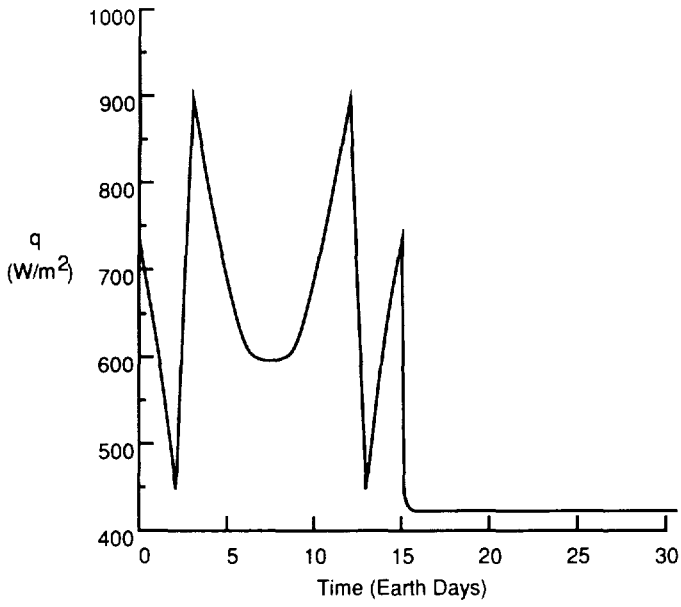

Fig. 13. Rejection capability of the radiator over the lunar day for a two-loop cascaded vapor cycle system in stagewise operation.

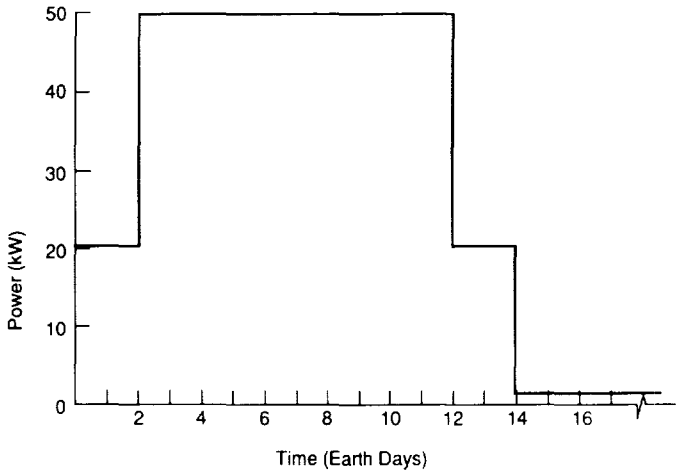

Fig. 14. Initial phase power summary for transportation and rejection systems.

TABLE 6. Radiator area requirements for the initial phase.

Time (Earth Days)	T_{rad}(K)	Total Q (kW)	Minimum q (W/m^2)	Maximum Area (m^2)	Maximum q (W/m^2)	Minimum Area (m^2)
0-2	311	115.5	450	257	750	154
3-11	360	145.0	600	242	900	161
12-14	311	115.5	450	257	750	154
15-28	262	95.0	420	226	420	226

over design level and by opening the louvers during design level operation. The standard spacecraft louvers are usually actuated by temperature-sensitive bimetallic springs that contract or expand in response to temperature differences from a single baseline temperature. For lunar base application, this actuation technique would not be acceptable because of the multiple temperature ranges in which the radiators must operate. Consequently, some type of electrically controlled actuator could be used.

An alternative concept, the variable conductance heat pipe radiator, could help control the rejection capability by controlling the actual amount of radiator surface area being used to reject heat. The concept consists of a heat pipe radiator filled with an appropriate working fluid connected to a large reservoir of inert gas that is pressurized to the saturation vapor pressure of the working fluid at the appropriate operating temperature (*Dunn and Reay,* 1978). If the heat input should rise from the design level, a resulting slight rise in temperature would increase the pressure of the working fluid. The working fluid would push inert gas back into the reservoir, thus exposing more radiator area for heat rejection, which would allow the temperataure to restabilize. If the heat input were reduced, the opposite effect would occur, that is, the radiator rejection area would decrease. An increase in rejection capability as a result of reduced external sink temperature or increased radiator temperature would also produce a reduction in active radiator rejection area. This reduction would then prevent imbalances by reducing the heat actually rejected to the appropriate levels. Since the rejection system was designed to function at three different operating temperatures (resulting from stagewise operation), the inert gas pressure must be adjusted to match the changing saturation vapor pressure of the working fluid at these different temperatures. This could be done by heating the inert gas using electrical or other types of heaters.

Heat Rejection System Design Estimates

The weight, volume, and power were calculated for the transport and rejection systems at the South Pole and Lacus Veris. In both cases, the transport system results included the bus heat exchangers, working fluid, and the lines shown in Fig. 6 plus an extra 10.0 m of lines out to the radiators. The transport lines were aluminum and were sized to accommodate the growth phase heat load (201 kW) when initially installed. The system also included a redundant set of lines for each temperature loop, pump packages, disconnects, valves, and sensors. In both cases, the rejection system was designed to evolve along with the increasing heat loads of the base. The rejection summary results included the radiator panels, clamp mechanisms, and the bus/radiator heat exchangers.

System design estimates at the South Pole. The space station heat rejection and transport technologies could be easily adapted for a lunar base located on the South Pole. The transportation system would be separate, pumped, two-phase ammonia loops operating at 2°C and 21°C. The rejection system estimates included a horizontal ammonia heat pipe radiator that provides a nearly constant heat flux during the lunar day and night (Figs. 7a,b). No rejection enhancement techniques were required. The system summaries are shown in Table 7. The Emulation-Simulation Thermal Control Model program was used to size the transport lines (*Hall et al.,* 1986; *Colwell and Hartley,* 1986). The weight and volume of the extra equipment in the transport system, such as the bus heat exchangers, insulation, valves, and pump packages, were determined using JSC's internal thermal control database for Phase B of the space station. The heat rejection system was also sized using data from JSC. This configuration could be used for base locations more than 70° from the equator; however, the system estimates would increase as the site moves farther from the pole.

System design estimates at the lower latitudinal regions. A two-loop cascaded VCS was selected for use at Lacus Veris with the space station ammonia heat pipe radiators as shown in Fig. 14. Each VCS was sized to accommodate 100 kW. The initial phase included one vapor cycle system and the growth phase included two vapor cycle systems. The VCS estimates included the compressor, evaporator, and the subcooler, plus the interstage line and the Freon 11 working fluid. The heat was transported from the modules to the rejection system by a single-temperature two-phase Freon 12 loop operating at -3°C. A vertical radiator oriented parallel to the solar ecliptic was selected because of the larger heat rejection capability obtainable for each stage temperature. Variable conductance heat pipes may be required to provide a more constant flux from the radiators; however, they were not included in these estimates. Evaporator and compressor bypass loops will be used for stagewise operation. The system summaries are shown in Table 8. The heat pump system estimates were obtained from the Sunstrand Corporation. The other system components were sized as discussed in the previous section. This system would also be adequate for other lower latitude base locations, with the estimates decreasing as the latitudes increase.

TABLE 7. Transport and rejection summary for initial and growth phases at the South Pole.

Phase		Weight (kg)	Volume (m^3)	Power (kW)
Initial				
Transport	2°C	696	8	0.33
	21°C	825	9	0.33
Rejection	2°C	1,319	4	0
	21°C	2,167	6	0
Total		5,007	27	0.66
Growth				
Transport	2/oC	1,518	17	0.66
	21°C	1,755	19	0.66
Rejection	2°C	2,920	8	0
	21°C	4,488	13	0
Total		10,681	57	1.32

TABLE 8. Transport and rejection summaries for the initial and growth phases at lower latitudinal regions.

Phase	Weight (kg)	Volume (m^3)	Power (kW)
Initial			
Heat pump	75	1	50.0
Transport	902	7	0.33
Rejection	3338	10	0
Total	4315	18	50.33
Growth			
Heat pump	150	2	100.0
Transport	2044	15	0.66
Rejection	6979	21	0
Total	9173	38	100.66

CONCLUDING REMARKS

A lunar base thermal control conceptual design derived from space station technology has been presented. The impact of landing site selection for both a South Pole site and low latitude sites was discussed. Alternate technologies were identified for those areas where space station technologies were not compatible with the lunar environment. Lunar resources that showed potential to enhance the thermal control concept were evaluated.

The lunar regolith was used as an insulator to minimize heat transfer from the base modules to the lunar environment. Space station acquisition technology was adequate for a base located at the South Pole or near the equator, whereas space station transport and rejection technology could only be adapted for a base at the South Pole. Lower latitudinal base sites will require alternate heat rejection techniques to accommodate the high environment sink temperatures encountered near the equator. A vapor cycle system was selected to provide this function. Conceptual designs were formulated and include weight, power, and volume estimates.

APPENDIX: PASSIVE THERMAL CONTROL ANALYSIS

The module's passive thermal control capability was evaluated to determine if the space station's multilayer insulation (MLI) will adequately protect the habitable areas from the lunar environment. The space station modules were assumed to be protected with MLI having an α/ϵ ratio of 0.8/0.8 (*NASA,* 1984) and an average thermal conductance between 0.16 W/m^2-K at 310 K and 0.05 W/m^2-K at 225 K (from Apollo correlation). Three cases were considered to determine if the space station's insulation would prevent large heat gains into the module during the lunar day and prevent large heat losses from the modules during the lunar night.

Case One

For case one, the module was assumed to be protected under an aluminum supporting structure with 2 m of regolith on top. The system was modeled as concentric cylinders to simplify calculations (Fig. A-1). Calculations using this geometry will provide conservative results. In this case the entire surface area of the "soil shell" around the module will experience the extreme day/night temperature variations, whereas, when actually deployed on the Moon, only half of the module's "soil shell" will experience the temperature extremes. The other half will experience the more benign temperature environment several meters below the lunar

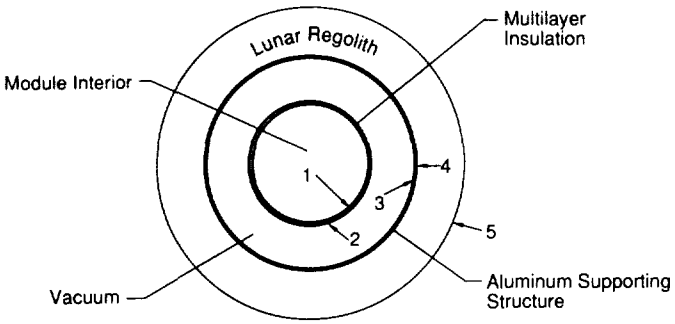

Fig. A-1. Concentric approximation for a lunar module under an aluminum structure and lunar regolith.

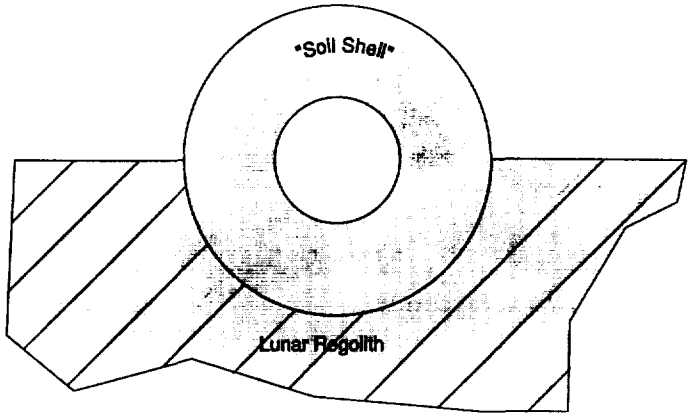

Fig. A-2. Actual environment of module's "soil shell."

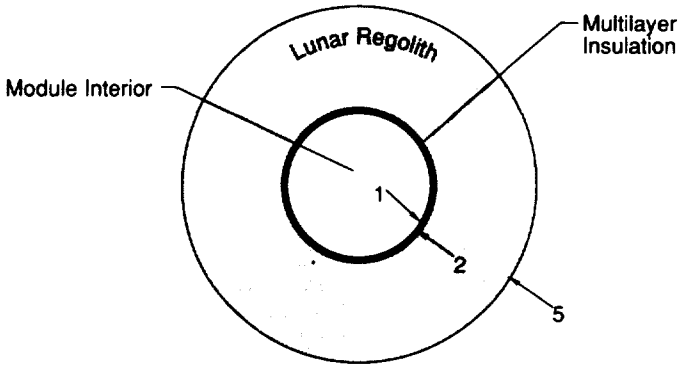

Fig. A-3. Concentric approximation for a lunar module buried directly under the lunar surface.

surface (Fig. A-2). The following equations were derived to determine the maximum heat exchange between the module and the environment at steady state

$$Q = 2\pi r_1 Hh(T_1 - T_2) = \frac{2\pi r_1 H\sigma(T_2^4 - T_3^4)}{\frac{1}{\epsilon_2} + \frac{r_1}{r_3}\left(\frac{1}{\epsilon_3} - 1\right)} =$$

$$\frac{2\pi Hk_{Al}(T_3 - T_4)}{\ln \frac{r_4}{r_3}} = \frac{2\pi Hk_{reg}(T_4 - T_5)}{\ln \frac{r_5}{r_4}}$$

where T_1 equals 294 K and T_5 equals either 374 K near the equator or 120 K during the lunar night. Solving for T_2, T_3, and T_4 yields a heat gain of 0.08 kW at lunar noon and a heat loss of 0.17 kW at night. These amounts of heat gain and heat loss are negligible compared to the estimated heat loads already in a habitation or laboratory module (0.3% and 0.7% of the 25-kW load, respectively). Thus, in this system the space station's MLI coupled with lunar regolith will provide adequate protection.

Case Two

In this case, the module was assumed to be buried 2 m directly below the lunar surface. Again, the system can be modeled as concentric cylinders (Fig. A-3). The following equation was derived to determine the maximum heat exchange between the module and the environment at steady state

$$Q = 2\pi r_1 Hh(T_1 - T_2) = \frac{2\pi Hk_{reg}(T_2 - T_5)}{\ln \frac{r_5}{r_1}}$$

where T_1 equals 294 K and T_5 equals either 374 K at noon near the equator or 120 K during the lunar night. The compressive force of the regolith on the MLI may significantly increase its thermal conductance and, therefore, decrease its insulating capability. Thus, it was assumed that T_2 approaches T_1, resulting in a maximum heat gain at noon of 0.05 kW and a maximum heat loss at night of 0.11 kW. Again, the heat gain and loss are negligible compared to the heat loads already acquired in a habitation or laboratory module (0.2% and 0.4%, respectively); therefore, the space station's MLI coupled with lunar regolith will provide adequate protection.

Case Three

A third case must be considered, where a module is directly on the surface and not covered by any lunar regolith. An example of this situation was the observatory that would be on the surface. The following equation was derived to determine the maximum exchange between the module and the environment at steady state

$$Q = 2\pi r_1 Hh(T_1 - T_2) = 2\pi r_1 H\sigma\epsilon_2(T_2^4 - T_{sink}^4)$$

where T_1 equals 294 K and T_{sink} equals either 358 K at noon near the equator or 98 K during the lunar night. Solving for T_2 gives a maximum heat gain of 2.2 kW and a maximum heat loss of 1.7 kW in the lower latitudinal region. These loads are 7% and 9%, respectively, of the module's total heat load; therefore, extra air temperature control will be needed during the hottest parts

of the lunar day and during the night to provide the crew with a comfortable environment. At the South Pole T_1 equals 294 K and T_{sink} equals 285 K during maximum solar flux or 98 K during the lunar night. The module will lose heat over the entire lunar day/night, with a maximum heat loss of 1.7 kW during the lunar night. The maximum heat loss is 7% of a module's total heat load; therefore, extra air temperature control will be needed.

Acknowledgments. The authors wish to express appreciation to the Sundstrand Corporation for their help in the development of the lunar heat pump system.

REFERENCES

Agrawal B. N. (1986) *Design of Geosynchronous Spacecraft*. Prentice-Hall, Englewood Cliffs. 459 pp.

Colwell G. T. and Hartley J. G. (1988) *Development of an Emulation-Simulation Thermal Control Model for the Space Station Application*. NAG-1-551. 88 pp.

Dallas T., Diaguila A. J., and Saltsman J. F. (1971) *Design Studies on the Effects of Orientation, Lunation, and Location on the Performance of Lunar Radiators*. NASA TM-X-1846. 40 pp.

Dalton C. and Hohmann E., eds. (1972) *Conceptual Design of a Lunar Colony*. Univ. of Houston, Houston. 529 pp.

Duke M. B., Mendell W. W., Roberts B. B. (1985) Strategies for a permanent lunar base. In *Lunar Bases and Space Activities of the 21st Century* (W. W. Mendell, ed.), pp. 57-68. Lunar and Planetary Institute, Houston.

Dunn P. D. and Reay D. A. (1978) *Heat Pipes*, 2nd edition. Pergamon, Oxford. 334 pp.

Hall J. B., Colwell G. T., and Hartley J. G. (1986) Evaluation of space station thermal control techniques. *Proc. Intersoc. Conf. Environ. Sys. 16th*, SAE Paper 860998. 16 pp.

MacKay D. B. (1963) *Design of Space Power Plants*. Prentice Hall, Toronto. 322 pp.

NASA (1984) *Space Station Reference Configuration Description*. JSC Publ. No. 19989, NASA Johnson Space Center, Houston. 786 pp.

NASA (1985) *Space Systems Technology Model*, 6th edition. NASA, Washington, DC.

Ride S. K. (1987) *Leadership and America's Future in Space: A Report to the Administrator*. U.S. Govt. Printing Office, Washington, DC. 63 pp.

Stimpson L. and Lucas J. W. (1972) Lunar thermal aspects from Surveyor data. In *Thermal Characteristics of the Moon, Vol. 28* (J. W. Lucas, ed.), pp. 121-150. MIT, Boston.